PNAS RESEARCH ARTICLE | CELL BIOLOGY OPEN ACCESS

Fra-2 controls the response to the KRAS inhibitor MRTX-1133 in pancreatic ductal adenocarcinoma

Erika Testa[a,1], Clara Dezi[a,1], Francesca Lovat[b], Geny Piro[c], Carmine Carbone[c], Marina Capece[b], Giovanni Nigita[b], Erisa Putro[a], Elisabetta Di Renzi[a], Alessandra Simeone[a], Luca Reggiani Bonetti[d], Roberto Cirombella[a], Paolo Magistri[e], Vincenzo Corbo[f], Davide Pasini[f], Barbara Belletti[g], Gustavo Baldassarre[g], Andrea Vecchione[a], Carlo M. Croce[b,2,3], and Gian Luca Rampioni Vinciguerra[a,b,2,3]

Affiliations are included on p. 8.

Contributed by Carlo M. Croce; received January 16, 2026; accepted February 9, 2026; reviewed by Michele Carbone and Gary S. Stein

KRAS mutations are a hallmark of pancreatic ductal adenocarcinoma (PDAC), driving tumor initiation and progression in the vast majority of cases, with KRAS^{G12D} being the most prevalent variant. Recent advances have led to the development of mutation-specific KRAS inhibitors (KRASi), yet their clinical impact is hindered by the rapid onset of drug resistance. In this study, we identify Fos-related antigen-2 (Fra-2), a stress-responsive transcription factor of the AP-1 family, as a key mediator of adaptive resistance to the KRAS^{G12D} selective inhibitor MRTX-1133. Using a combination of established PDAC cell lines, xenograft models, and patient-derived organoids, we demonstrate that Fra-2 expression is consistently upregulated following MRTX-1133 treatment. Functional assays reveal that Fra-2 overexpression promotes resistance by reprogramming the transcriptional landscape, directly enhancing mTOR expression and signaling. Consistently, FRA2 and MTOR levels strongly correlate in PDAC patient samples. Collectively, these findings uncover a mechanistic interplay between Fra-2 and the mTOR pathway in MRTX-1133-resistant PDAC, highlighting that targeting Fra-2 may represent a valuable approach to enhance the efficacy of KRASi.

pancreatic cancer | Fra-2 | KRAS inhibitors | MRTX-1133 | mTOR pathway

Pancreatic ductal adenocarcinoma (PDAC) is a deadly malignancy, heavily resistant to current therapies, and projected to become the second leading cause of cancer-related death in the coming years (1). The 5-year survival rate remains dismal at 12%, one of the lowest among all cancers (2). In fact, nearly 80% of patients are ineligible for surgery, leaving systemic therapy as the mainstay of treatment (3, 4). However, PDAC rapidly acquires resistance to standard cytotoxic regimens such as FOLFIRINOX and gemcitabine-based therapies, which nonetheless remain first-line options. Targeted treatments are limited, with PARP inhibitors showing benefit only in a small subset of patients (5, 6).

Recently, the development of mutant-specific KRAS inhibitors (KRASi) has opened therapeutic perspectives (7). The first-in-class KRAS^{G12C} inhibitor AMG510 (sotorasib) showed promising efficacy in advanced lung cancer harboring this mutation (8, 9), paving the way for a new generation of KRAS-targeted therapies. In PDAC, however, KRAS^{G12C} mutations are relatively uncommon, whereas KRAS^{G12D} is the most prevalent variant, occurring in nearly 46% of patients (10). This molecular dependency has fostered the development of allele-specific KRAS^{G12D} inhibitors, with MRTX-1133 (hereafter MRTX) emerging as a first-in-class compound (11). In multiple preclinical models, MRTX markedly suppressed MAPK signaling downstream of KRAS, thereby impairing PDAC growth (12). Despite these advances, accumulating evidence indicates the rapid emergence of resistance to KRASi across different models, significantly limiting their clinical utility (13).

Fra-2, a member of the AP-1 transcription factor family, is recognized as an immediate early gene and is frequently dysregulated in several human malignancies (14–16). Fra-2 is rapidly activated by diverse stimuli including inflammation, hypoxia (17), serum deprivation (18), and oxidative stress (19). This feature is especially well-documented in PDAC, where Fra-2 enhances the tumor ability to thrive and progress in nutrient restriction (18). Previous studies have implicated Fra-2 in drug resistance across multiple tumor types, including lung cancer (20), ovarian cancer (19), and squamous cell carcinoma (15). Nevertheless, the contribution of Fra-2 to the development of resistance in PDAC remains largely unexplored, representing a critical gap in our current understanding.

Herein, we explore the possible involvement of Fra-2 in the cell stress response under drug administration. We report that Fra-2 is activated by different compounds and orchestrates the transcriptional mechanisms driving the MRTX resistant phenotype in PDAC.

Significance

KRAS mutations are present in the majority of pancreatic ductal adenocarcinomas (PDAC) and are key drivers of tumor progression. Although mutation-specific KRAS inhibitors (KRASi) have shown encouraging clinical activity, their therapeutic benefit is limited by the insurgence of resistance. Here, we hypothesized that the stress-response mediator Fra-2 contributes to this resistance. We show that treatment with the KRASi MRTX-1133 induces Fra-2 overexpression, leading to transcriptional rewiring that includes regulation of mTOR expression. Importantly, combination therapy targeting Fra-2 significantly improves the efficacy of KRASi. These findings provide mechanistic insight into the recurrent activation of the mTOR pathway in MRTX-1133–resistant PDAC and identify Fra-2 as a promising therapeutic target for combination strategies.

Reviewers: M.C., University of Hawai'i Cancer Center; and G.S.S., University of Vermont.

The authors declare no competing interest.

[1]E.T. and C.D. contributed equally to this work.

[2]C.M.C. and G.L.R.V. contributed equally to this work.

[3]To whom correspondence may be addressed. Email: carlo.croce@osumc.edu or gianluca.rampionivinciguerra@uniroma1.it.

This article contains supporting information online at https://www.pnas.org/lookup/suppl/doi:10.1073/pnas.2601788123/-/DCSupplemental.

Published April 29, 2026.

Results

Fra-2 Expression Is Upregulated Under Drug Administration and Contributes to KRASi Response. As previously reported, Fra-2 is involved in the cellular stress response to hypoxia and nutrient deprivation in PDAC (17, 18). We have shown that Fra-2 is activated by nutrient deprivation and, in turn, initiates a complex adaptive response involving the IGF1R pathway, ultimately promoting cell survival and tumor growth under unfavorable metabolic conditions (18). To investigate whether Fra-2 upregulation could also be triggered by drug treatment, we tested agents commonly used in PDAC therapy, namely cisplatin and gemcitabine (2). Both drugs induced a marked upregulation of Fra-2 in PDAC cells (Fig. 1 *A* and *B*).

To evaluate the effect of MAPK pathway inhibition on Fra-2 expression, cells were exposed to increasing concentrations of the MEK inhibitor U0126. Dose–response curve and western blot analysis showed a dose-dependent upregulation of Fra-2 (Fig. 1 *C* and *D*). Moreover, chromatin immunoprecipitation (ChIP) analysis revealed increased Fra-2 occupancy at the IGF1R promoter (Fig. 1*E*), a known transcriptional target (18), suggesting a sustained transcriptional activity under MEK inhibition. Consistently, treatment with the KRASi MRTX also enhanced Fra-2 expression in PDAC cells (Fig. 1*F*). Functionally, Fra-2 contributed to drug response, as FRA2 knockout ($FRA2^{KO}$) AsPC-1 cells displayed increased sensitivity to MRTX compared with controls (Fig. 1*G*).

To further examine whether Fra-2 is involved in acquired resistance to MRTX, we generated a KRAS inhibitor–resistant (KRASi-res) model by exposing AsPC-1 cells, a highly aggressive PDAC cell line derived from ascitic fluid (21), to progressively increasing concentrations of MRTX (Fig. 1*H*). After one month, cells were adapted to 50 nM MRTX, and the resistant population was maintained under continuous drug pressure. Dose–response analysis confirmed a resistant phenotype compared to parental cells (Fig. 1*I*), while western blotting demonstrated a robust increase in Fra-2 protein expression (Fig. 1*J*).

Collectively, these results identify Fra-2 as a stress-responsive effector induced by drug treatment in PDAC cells and implicate it in both primary and acquired responses to MRTX.

Inhibition of Fra-2 Transcriptional Activity Increases MRTX Efficacy In Vivo. We previously demonstrated that AP-1 targeting, *via* Fra-2 blockade, represents a valid approach to overcome drug resistance in other malignancies (20). To evaluate whether Fra-2 inhibition could synergize with MRTX, we established a xenograft model by injecting wild-type ($FRA2^{WT}$) and $FRA2^{KO}$ AsPC-1 cells into the flanks of nude mice (Fig. 2*A*). Once tumors became palpable, mice were randomly assigned to four groups and treated for 20 d with MRTX (10 mg/kg, twice daily), the AP-1 inhibitor T-5224 (30 mg/kg, once daily), or their combination (Combo). At the study endpoint, mice were killed and tumors collected for further analyses.

In this tumor model, T-5224 administration had minimal impact on tumor progression in either genotype, suggesting that Fra-2 inhibition had no impact per se (Fig. 2 *B* and *C*). By contrast, MRTX treatment reduced tumor growth more effectively in $FRA2^{KO}$ xenografts than in $FRA2^{WT}$ counterparts ($P < 0.05$ *versus* $P < 0.001$). Importantly, combining MRTX with T-5224 markedly enhanced the antitumor efficacy of KRASi in $FRA2^{WT}$ tumors, whereas no additional benefit was observed in $FRA2^{KO}$ tumors (Fig. 2 *B* and *C*).

Histological analyses confirmed that cotreatment with T-5224 significantly reduced cell proliferation in $FRA2^{WT}$ tumors but not in $FRA2^{KO}$ tumors (Fig. 2 *D* and *E*). Consistently, western blot analyses revealed that MRTX treatment induced Fra-2 overexpression in $FRA2^{WT}$ tumors, while the addition of T-5224 further decreased levels of p-ERK1/2 compared to MRTX alone (Fig. 2*F*).

Taken together, these results demonstrate that AP-1 inhibition enhances the therapeutic efficacy of MRTX in PDAC and that this effect is mediated *via* Fra-2 targeting.

Fra-2 Promotes mTOR Pathway Enrichment in Response to MRTX. Data collected so far indicated that KRASi triggers Fra-2 upregulation that, in turn, modulates drug sensitivity. To elucidate how Fra-2 was mechanistically linked to KRASi response, we investigated the transcriptomic reprogramming induced by MRTX, comparing KRASi-res (Fig. 1*H*) and $FRA2^{KO}$ AsPC-1 cells treated with MRTX (50 nM) *versus* untreated parental and $FRA2^{KO}$ cells (22) (Fig. 3 *A* and *B*). Fra-2–proficient cells displayed more modulated genes relative to $FRA2^{KO}$ cells (Fig. 3 *A* and *B*), indicating that Fra-2 critically modulated the transcriptome upon MRTX. Pathway enrichment analysis (IPA®) of genes specifically altered in KRASi-res compared to $FRA2^{KO}$ cells under MRTX revealed 20 pathways selectively altered in the presence of Fra-2 ($-\log P > 2$, $|\text{z-score}| > 1$) (Fig. 3*C*). Among them, MRTX treatment enriched the mTOR signaling pathway, a known driver of KRASi resistance in PDAC (13), in a Fra-2-dependent manner. To identify Fra-2–dependent targets involved in this process, we intersected the gene sets obtained from transcriptomic analyses and focused on genes upregulated in KRASi-res cells, compared to both parental and $FRA2^{KO}$ cells, that remained unchanged in MRTX-treated $FRA2^{KO}$ cells (Fig. 3*D*). This approach yielded a core set of 1318 Fra-2–dependent genes, which included the MTOR gene itself. Consistently, RT-qPCR from xenografted tumors showed MTOR upregulation in $FRA2^{WT}$, but not $FRA2^{KO}$, tumors after MRTX, with expression returning to baseline upon T-5224 cotreatment (Fig. 3*E*), underscoring the interplay between Fra-2 and mTOR upon KRASi. Given these intriguing correlations and the in silico evidence, showing direct Fra-2 binding to the MTOR locus (FOSL2_A549_hg19_1, ENCODE Transcription Factor Targets dataset) (23), we hypothesized that MTOR might be a direct Fra-2 target under KRASi. Supporting this possibility, ChIP analysis showed enhanced Fra-2 binding to a motif upstream of the MTOR start codon (24) in KRASi-res compared to parental AsPC-1 cells (Fig. 3 *F* and *G*), thus highlighting a direct role of Fra-2 in driving MTOR expression under KRASi.

Fra-2 Drives mTOR Upregulation Under MRTX Administration in Patient-Derived Organoids of PDAC. Our results support a role for Fra-2 in modulating MTOR expression in PDAC cells exposed to KRASi. To assess whether this association also occurs in PDAC patients, we analyzed transcriptomic data from the TCGA dataset. A global expression analysis revealed widespread transcriptional dysregulation, with 15556 genes showing high expression and 22347 showing low expression across PDAC samples (Fig. 4*A*); notably, both FRA2 and MTOR were among the strongly overexpressed genes. To investigate the molecular networks potentially enriched by Fra-2 activity, we performed a Gene Set Enrichment Analysis (GSEA) (25) using Hallmark gene sets on genes positively associated with FRA2 expression in PDAC samples. This analysis revealed significant enrichment of pathways commonly involved in PDAC progression, including epithelial–mesenchymal transition and MYC targets, notably MTORC1 signaling (*SI Appendix*, Fig. S1). Consistently, direct comparison of FRA2 and MTOR transcript levels demonstrated

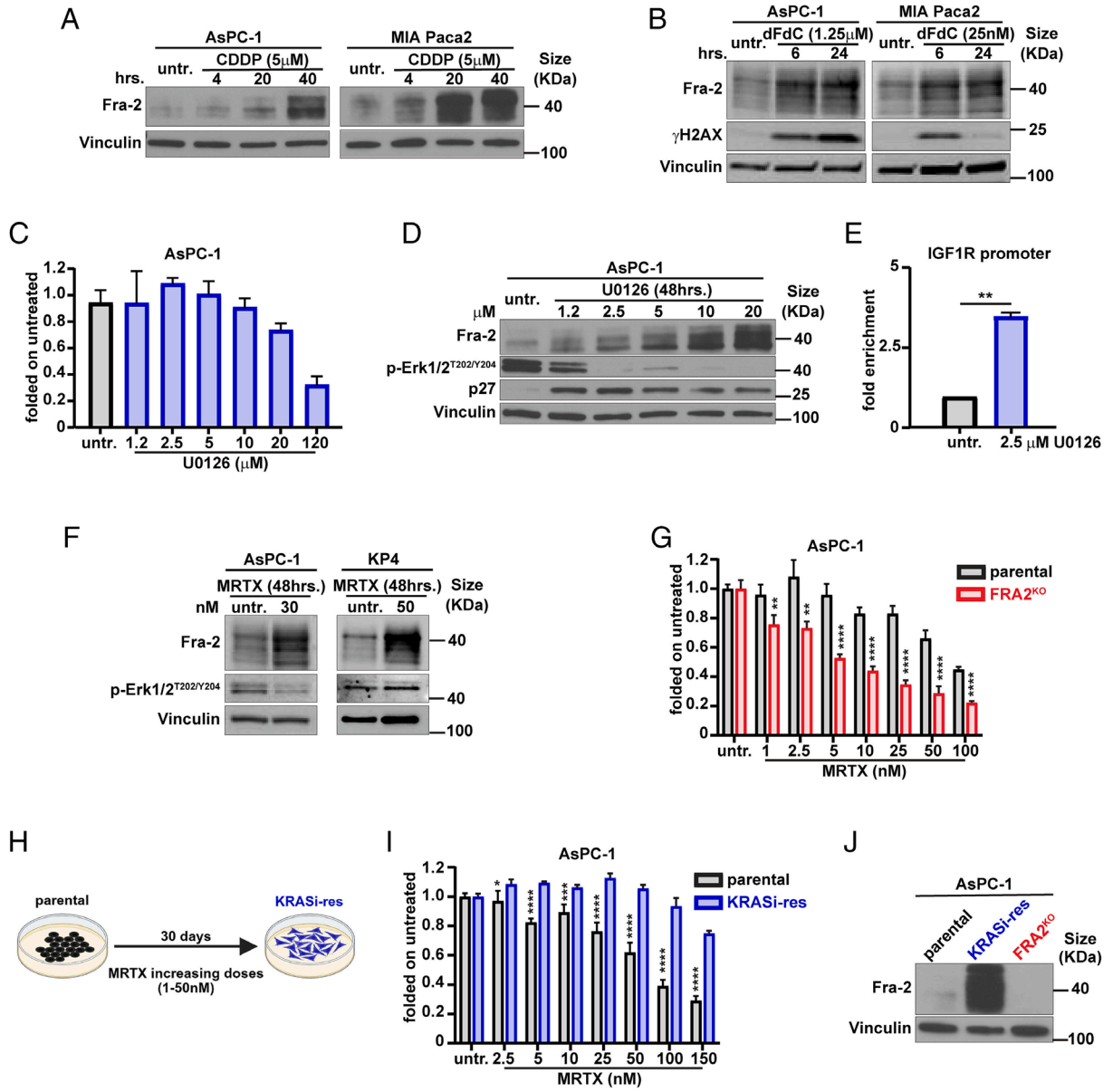

Fig. 1. Fra-2 expression is upregulated under drug administration and contributes to KRASi response. (*A* and *B*) Western blot analyses of Fra-2 protein levels in AsPC-1 and MIA Paca-2 cell lines treated with Cisplatin (CDDP) (*A*) or Gemcitabine (dFdC) (*B*) at the indicated concentrations and collected at the indicated time points (hours, h). Vinculin was used as loading control, while γH2AX served as a DNA damage marker of dFdC efficacy. (*C*) Dose–response curve of AsPC-1 cells treated with increasing concentrations of U0126. Data are collected after 48 h of treatment, are folded over the untreated cells, and represent the mean (±SD) from two independent experiments. (*D*) Western blot analysis of the indicated proteins in AsPC-1 cells treated with increasing concentrations of U0126 for 48 h. Vinculin was used as loading control, while p-ERK1/2 and p27 served as markers of U0126 activity. (*E*) Chromatin immunoprecipitation (ChIP) assay of Fra-2 bound to the IGF1R promoter in AsPC-1 cells following treatment with 2.5 μM of U0126. Data represent the mean (±SD) of two independent experiments. Unpaired *t* test was used for statistical analyses and asterisks indicate significant differences compared to the untreated condition. $^{**}P < 0.01$. (*F*) Western blot analyses of the indicated proteins in AsPC-1 and KP4 cells treated with the indicated concentration of MRTX for 48 h. Vinculin was used as loading control. (*G*) Dose–response curve of parental and FRA2 knock-out ($FRA2^{KO}$) AsPC-1 cells treated for 72 h with increasing doses of MRTX. (*H*) Schematic representation of the experimental workflow used to induce KRAS inhibitor resistance in AsPC-1 cells. Cells were continuously treated with increasing doses (from 1 to 50 nM) of MRTX for 30 d. The isolated resistant population was then maintained in a medium containing 50 nM of MRTX. Resistant phenotype was confirmed by cell viability assay as described in *I*. Created with BioRender.com. (*I*) Dose–response curve reporting the cell viability of parental and MRTX resistant (KRASi-res) AsPC-1 cells, treated for 72 h with increasing doses of MRTX. (*J*) Western blot analysis of lysates from the same cells used for the experiments described in *G*–*I*. Vinculin was used as loading control. In *G* and *I*, cell viability was measured by MTS assay and data are folded over the untreated cells. Unpaired *t* test was used for statistical analyses and asterisks mark significant differences. $^{*}P < 0.05$; $^{**}P < 0.01$; $^{***}P < 0.001$; $^{****}P < 0.0001$.

a strong positive correlation across PDAC samples (Spearman r = 0.691; $P < 0.0001$; n = 147) (Fig. 4*B*). This finding was further validated in an independent internal cohort of 42 PDAC patients (*SI Appendix*, Table S1), which confirmed a significant correlation between FRA2 and MTOR expression (r = 0.4268, $P = 0.0048$) (Fig. 4*C*).

To corroborate these findings in a translational setting, we next employed patient-derived organoids (PDOs) from treatment-naïve, annotated, primary PDAC (*SI Appendix*, Table S2). Transcriptomic profiling of four PDOs revealed distinct FRA2 expression (Fig. 4*D*). We chose two PDOs with divergent FRA2 levels and minimal baseline expression of the mTORC1 pathway (Fig. 4*E*) to explore whether KRASi influenced the Fra-2/mTOR axis. In line with cellular and xenograft models, MRTX markedly increased FRA2 expression in PDO#23^{FRA2low}, accompanied by parallel MTOR induction (Fig. 4*F*). In PDO#2^{FRA2high}, FRA2 levels

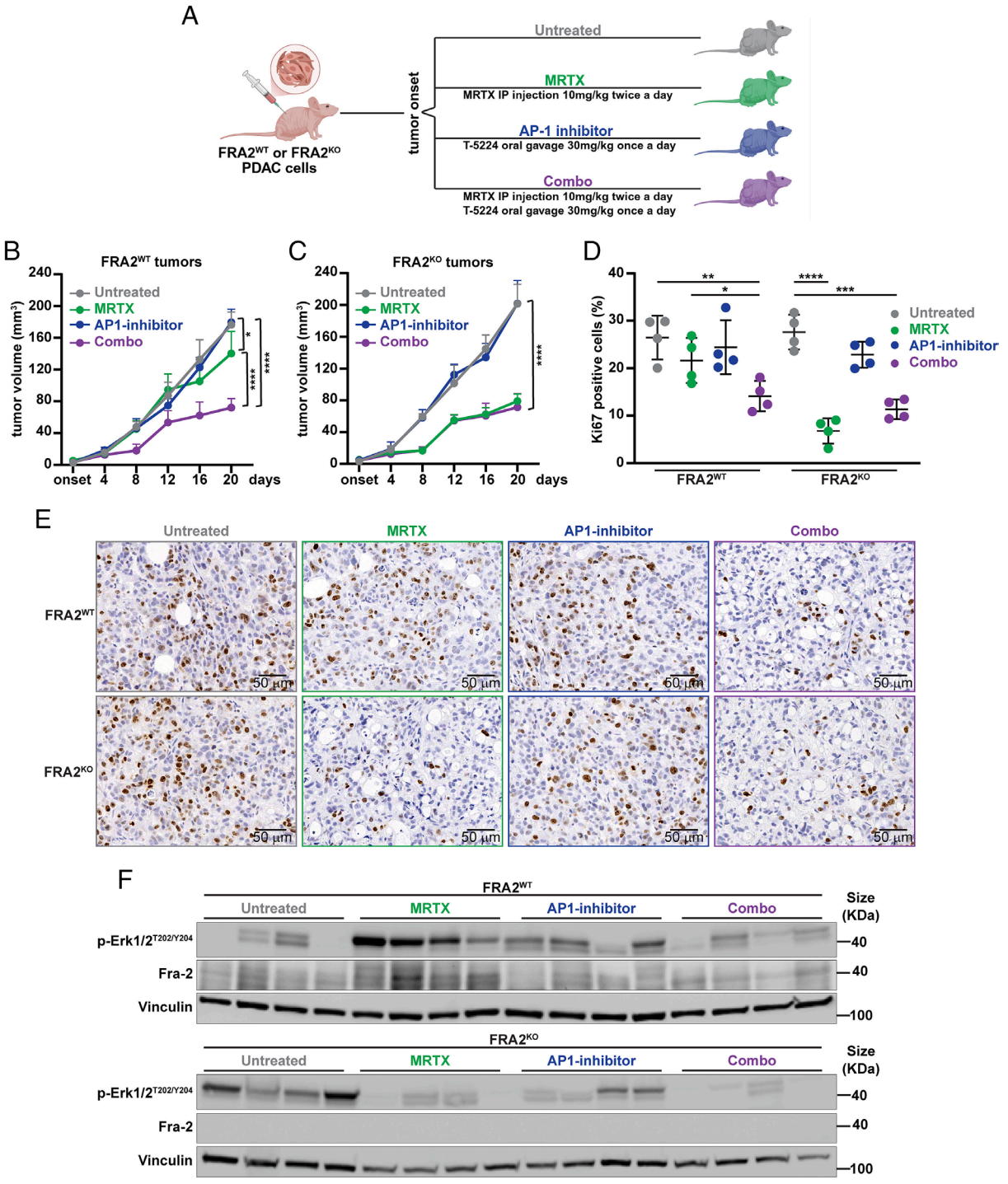

Fig. 2. Inhibition of Fra-2 transcriptional activity increases MRTX efficacy in vivo. (*A*) Schematic representation of the experimental workflow used for the evaluation of the tumor growth and the response to the KRASi MRTX in mice xenografted with PDAC cells. Nude mice were injected in the flank with either FRA2^{WT} or FRA2^{KO} AsPC-1 cells. Once tumor onset was established, mice were randomly subdivided in four different cohorts and treated for 20 d with vehicle, MRTX, or the AP-1 inhibitor T-5224, alone or in combination (Combo), as indicated. (*B* and *C*) Graphs reporting the growth rate of FRA2^{WT} (*B*) and FRA2^{KO} (*C*) tumors (n = 4 tumor/group), treated as described in *A*. Data represent the mean (±SD) of 4 tumor/group and two-way ANOVA was used to verify statistical significance. *$P < 0.05$; ****$P < 0.0001$. (*D*) Graph reports the percentage of Ki-67 positive cells in FRA2^{WT} and FRA2^{KO} tumors treated as described above. Each dot represents the mean of Ki-67 percentage counted in four randomly selected high-power fields (40× magnification) for each tumor. Unpaired *t* test was used to assess the statistical significance. *$P < 0.05$; **$P < 0.01$; ***$P < 0.001$; ****$P < 0.0001$. (*E*) Typical images of Ki-67 expression evaluated by immunohistochemistry in FRA2^{WT} and FRA2^{KO} tumors explanted from mice treated as summarized in *A*. (*F*) Western blot analyses evaluating the expression of the indicated proteins in lysates from FRA2^{WT} (*Top*) and FRA2^{KO} (*Bottom*) tumors explanted from mice treated as indicated. Vinculin was used as loading control.

remained stable but MRTX still promoted significant MTOR upregulation (Fig. 4*G*), suggesting that Fra-2 can either be induced in response to KRASi or, when already highly expressed, altogether sustain its activation. Notably, cotreatment with T-5224 restored MTOR expression to baseline in both PDO models.

Discussion

The rapid emergence of resistance to conventional chemotherapy remains one of the major challenges in PDAC (1), prompting the search for novel selective inhibitors. In this context, the

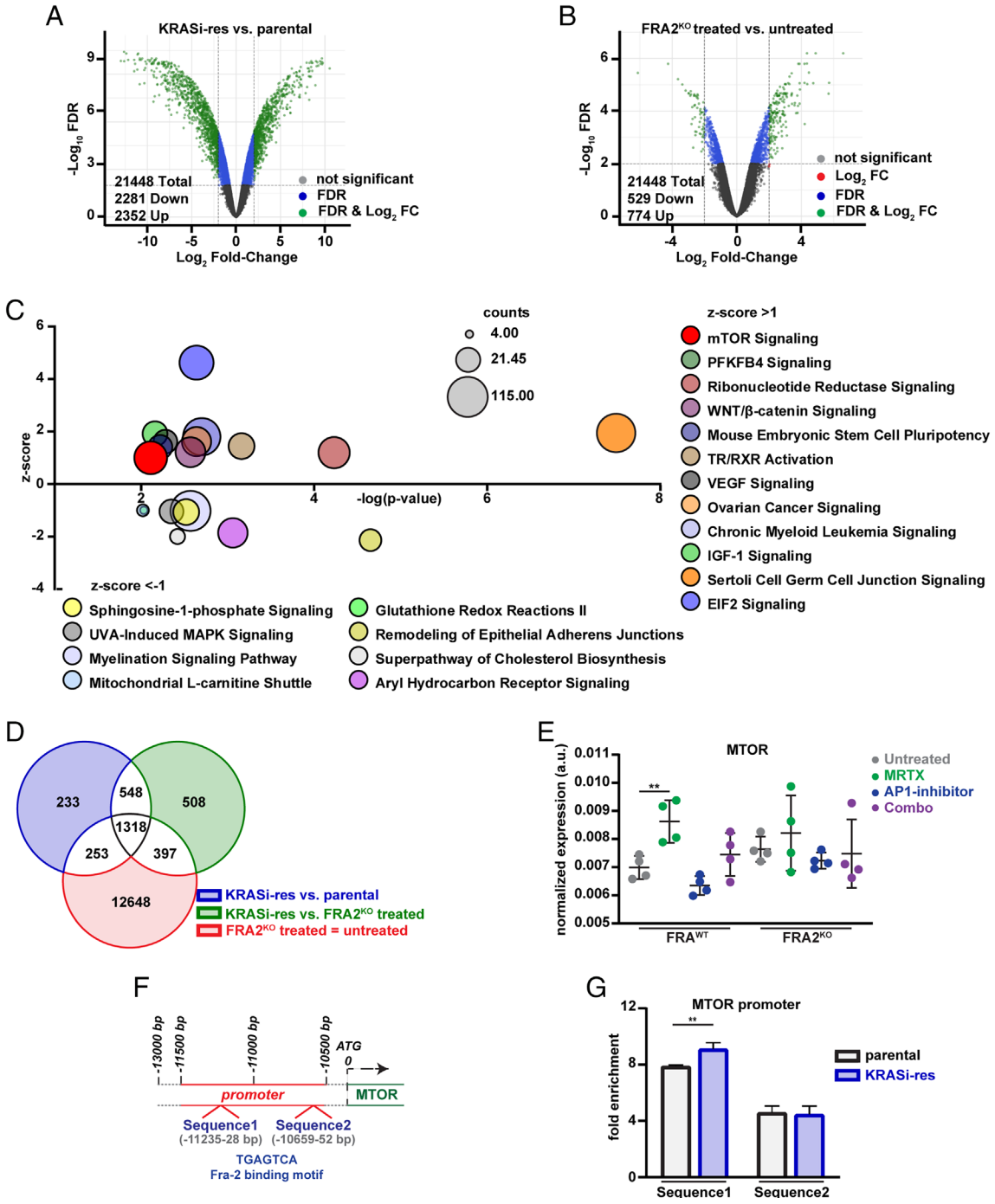

Fig. 3. Fra-2 promotes mTOR pathway enrichment under MRTX administration. (*A* and *B*) Volcano plots depicting KRASi-dependent gene expression changes upon MRTX administration in parental (*A*) and FRA2^{KO} (*B*) AsPC-1 cells as assessed by microarray-based transcriptomic profiling. Genes significant by both FDR (–log10 adjusted $P < 0.01$) and fold change (|log2FC| >2) are shown in green; FDR-only in blue; fold change–only in red; and nonsignificant in gray. (*C*) Bubble plot of molecular networks significantly modulated in Fra-2–proficient cells under KRASi. Data were derived from IPA® analysis of genes specifically altered in KRASi-res versus MRTX treated (50 nM) FRA2^{KO} AsPC-1 cells (–log *P*-value > 2, |z-score| > 1). Pathway activation state is indicated by the z-score (positive or negative enrichment). Bubble size represents the number of mapped genes, color indicates pathway category, and the axes display statistical significance (–log *P*-value) and activation (z-score). (*D*) Venn diagram showing differentially expressed genes (FDR <0.01, |FC| > 2) across three pairwise comparisons. Blue indicates genes upregulated in KRASi-res versus parental AsPC-1 cells (2352 genes). Green denotes genes upregulated in KRASi-res *versus* MRTX treated (50 nM) FRA2^{KO} cells (2771 genes). Red represents genes unaltered in FRA2^{KO} cells upon MRTX (14616 genes). The overlap reveals a core set of 1318 genes consistently associated with KRASi in a Fra-2–dependent manner. (*E*) Graph reporting the normalized expression of MTOR evaluated by RT-qPCR analysis in FRA2^{WT} and FRA2^{KO} tumors explanted from mice treated as indicated and described in Figure 2*A*. Each dot represents a different tumor. (*F*) Schematic representation of Fra-2-binding sequences on MTOR promoter. (*G*) Chromatin immunoprecipitation (ChIP) analysis of Fra-2 binding to consensus sequences within the MTOR promoter in KRASi-resistant (KRASi-res, blue) and parental (black) AsPC-1 cells. Data represent the mean (±SD) of three independent experiments. In *E* and *G*, unpaired *t* test was used to assess the statistical significance and asterisks. $^{**}P < 0.01$.

development of KRASi has opened avenues for therapeutic intervention (7). Nevertheless, PDAC cells quickly acquire resistant phenotypes, thereby limiting the long-term efficacy of these agents (26). Growing evidence from both the literature and our laboratory highlights the role of Fra-2 in mediating PDAC adaptability to microenvironmental cues (17, 18, 27). However, Fra-2 potential involvement in modulating therapeutic responses in PDAC remains unexplored.

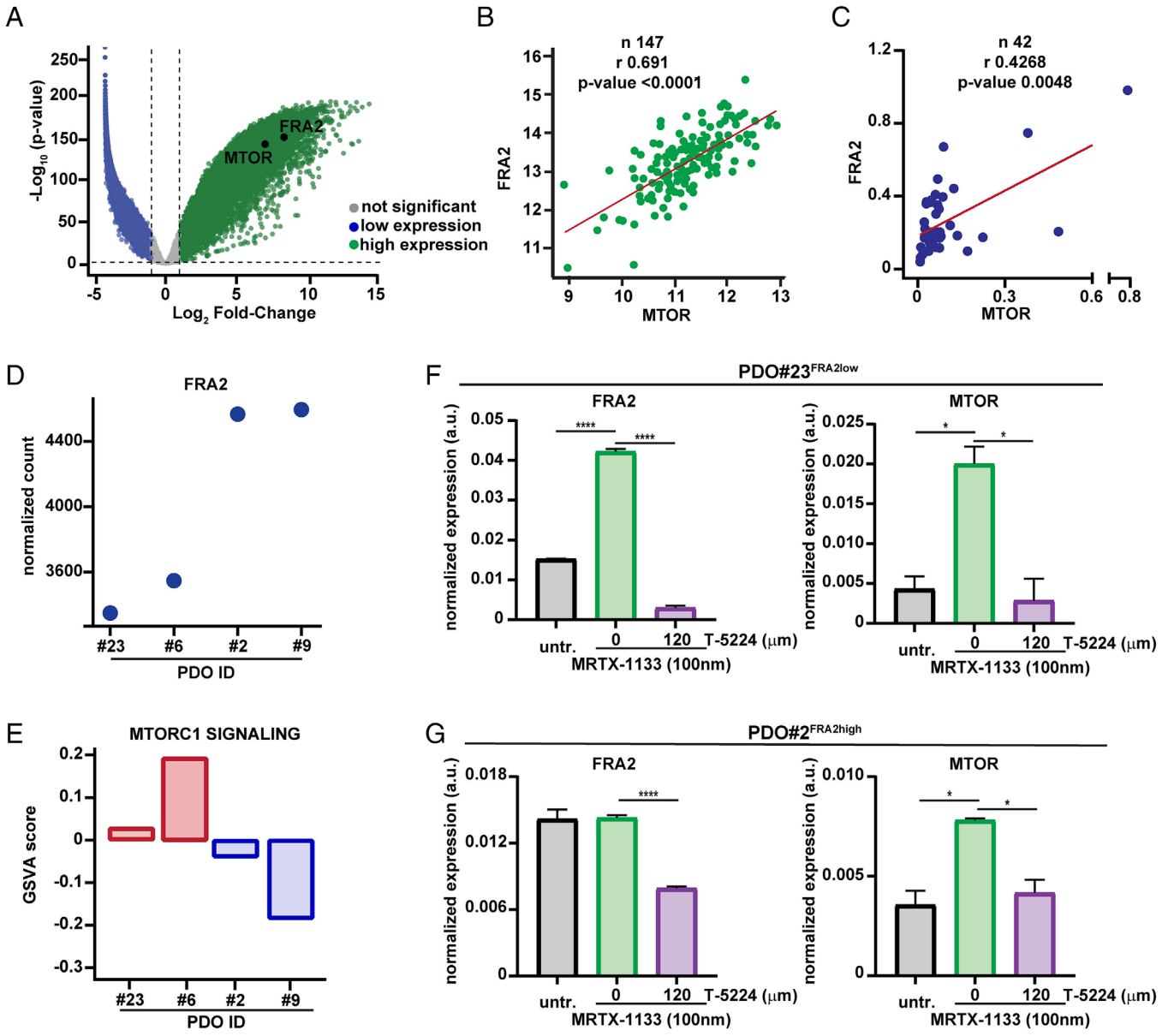

Fig. 4. Fra-2 modulates MTOR expression in MRTX–treated PDAC patient-derived organoids (PDOs). (*A*) Dot plot showing the results of the global gene expression analysis, which revealed widespread transcriptional dysregulation with highly expressed (n = 15556, in green) and lowly expressed (n = 22347, in blue) genes across PDAC samples from the TCGA dataset. FRA2 and MTOR expression levels are indicated by black dots. (*B* and *C*) Scatter plots representing the correlation of FRA2 with MTOR expression levels in PDAC samples from TCGA dataset (*B*) and an independent cohort of patients evaluated by RT-qPCR (*C*). The number of analyzed samples (n), the Spearman correlation value (r), and its significance (*P*-value) are reported in the graphs. (*D*) Graph showing normalized transcript counts of FRA2 across a set of four (#23, #6, #2, and #9) individual PDOs of PDAC. (*E*) Gene Set Variation Analysis (GSVA) scores for the "MTORC1 signaling" Hallmark gene set in individual PDO models. GSVA was performed on RNA-seq expression profiles from PDO samples #23, #6, #2, and #9 to quantify the relative enrichment of MTORC1 pathway activity. Positive scores (red bars) indicate higher pathway activation, whereas negative scores (blue bars) reflect lower activity compared to the cohort median. (*F* and *G*) Graphs showing the normalized expression of FRA2 and MTOR, evaluated by RT-qPCR analyses in PDO#23^{FRA2low} (*F*) and PDO#2^{FRA2high} (*G*) under MRTX administration (100 nM, 48 h), alone or in combination with the AP-1 inhibitor T-5224 (120 μM, 48 h). Data represent the mean (±SD) of two independent experiments and unpaired *t* test was used to assess significant differences. **P* < 0.05; ****P* < 0.001.

Here, we reveal that Fra-2 was consistently upregulated in PDAC cells upon gemcitabine and cisplatin treatment (Fig. 1*A*, B), as well as the MEK-inhibitor U0126 (Fig. 1*D*). Under MAPK-pathway blockade, Fra-2 increased its binding to the IGF1R promoter (Fig. 1*E*), a key driver of drug resistance in multiple cancers, including PDAC (28). Consistently, our previous observations showed that IGF1R overexpression is also a distinctive trait of the stress-tolerant phenotype mediated by Fra-2, further underscoring the importance of the Fra-2/IGF1R axis in PDAC adaptivity (18).

Focusing on KRASi, we found that MRTX treatment significantly increased Fra-2 levels (Fig. 1*F*) and reduced drug sensitivity (Fig. 1*G*). Fra-2 was also upregulated in an in vitro MRTX–resistant model (Fig. 1 *H–J*), indicating a potential link between Fra-2 activation and resistance. Recently, multiomics profiling of preclinical and patient-derived PDAC models has revealed that resistance to KRAS^{G12D} inhibition involves both acquired mutations and adaptive responses (13). While recurrent genetic alterations, including amplification of MYC, MET, EGFR, and CDK6 have been reported, evidence indicates that resistance rarely arises from secondary mutations (29). Rather, it is primarily driven by cellular plasticity, including epithelial–mesenchymal transition and mTOR signaling, with the molecular effectors orchestrating this adaptive rewiring remaining largely undefined (13). Within this framework,

our findings suggest that the transcription factor Fra-2 may act as a mediator of adaptive responses in PDAC cells exposed to KRASi.

Importantly, coadministration of the AP-1 inhibitor T-5224 enhanced the sensitivity of xenografted PDAC tumors to MRTX in a Fra-2-dependent manner (Fig. 2 *B*-*F*). In the literature, combination strategies have been proposed to enhance the efficacy of selective inhibitors in KRAS-dependent malignancies (29). Some studies have focused on targeting upstream interactors of the KRAS pathway (12, 30), while others have emphasized the concomitant blockade of ancillary pathways activated in response to KRASi, such as mTOR signaling (26, 31). Additional approaches underscore the role of non–cell-autonomous mechanisms, suggesting that combining MRTX with immune checkpoint inhibitors may further improve therapeutic efficacy (32, 33). Our findings suggest that targeting transcription factors may represent an additional strategy to enhance KRASi efficacy. Notably, they identify Fra-2 as a potential target and support the use of the AP-1 inhibitor T-5224 as a promising approach, in line with prior reports from our group and others (20, 34). Moreover, T-5224 was originally developed for the treatment of rheumatoid arthritis, and a phase II clinical trial demonstrated that its oral administration was not associated with serious adverse effects (35). These observations further underscore the translational relevance of our findings and support the feasibility of testing the combination of KRASi and T-5224 in patients.

Using an integrative approach, we investigated the transcriptional changes induced by MRTX in parental and FRA2^{KO} PDAC cells (Fig. 3 *A* and *B*). Fra-2–proficient cells showed a larger set of dysregulated genes, indicating that Fra-2 shapes both specific and broad molecular responses. Bioinformatic analyses confirmed a Fra-2–dependent rewiring of oncogenic programs (Fig. 3*C*), notably IGF1 signaling, further highlighting its role as a key downstream effector in PDAC. We also observed alterations in lipid metabolism and stress-related pathways, underscoring that drug resistance relies on compensatory signaling and metabolic adaptations. These mechanisms and their therapeutic implications warrant further investigation.

In this study, we investigated the regulatory role of Fra-2 in mTOR signaling, a crucial adaptive mechanism to MRTX resistance (13). Mechanistically, MRTX administration increased MTOR expression and enhanced Fra-2 binding to the MTOR promoter (Fig. 3 *E*–*G*), suggesting a direct regulation of MTOR transcription in response to KRASi. From a translational perspective, we observed a strong positive correlation between FRA2 and MTOR expression in both the TCGA dataset (Fig. 4*B*) and in an independent cohort of PDAC patients (Fig. 4*C*). Furthermore, in PDAC PDOs, MRTX administration induced MTOR expression, whereas cotreatment with T-5224 restored its basal levels, further supporting mTOR as a downstream target of Fra-2 activity (Fig. 4 *F* and *G*).

Taken together, these findings identify Fra-2 as a critical regulator of adaptive responses to KRASi and a contributor to the emergence of resistance in PDAC. Our data provide mechanistic insight into the mTOR signaling enrichment commonly observed in response to KRASi and open the possibility for combined strategies targeting Fra-2–dependent pathways to improve the efficacy of KRASi.

Materials and Methods

Patient Samples and Study Approval. Specimens from deidentified 42 treatment-naïve primary PDAC were collected at the Pathology Unit, Department of Diagnostic, Clinic and Public Health Medicine, University of Modena and Reggio Emilia, Modena, Italy. The study was approved by the Ethical Committee "Comitato Etico dell'Area Vasta Emilia Nord" of the University of Modena and Reggio Emilia, Italy (Prot. AOU #0019500/21), and by the Internal Review Board of The Ohio State University (IRB #2018C0131). The experiments conformed to the principles set out in the WMA Declaration of Helsinki and the Department of Health and Human Services Belmont Report. The fresh pancreatic (PDAC) tissues used to establish PDOs and associated clinical and follow-up data were collected under a study approved by the Integrated University Hospital Trust (AOUI) Ethics Committee (Comitato Etico Azienda Ospedaliera Universitaria Integrata): approval number 1911 (protocol number 61413, Prog 1911 on 19 September 2018).

Animal study approval. All animal experiments were performed in compliance with institutional guidelines and approved by the Institutional Animal Care and Use Committee (IACUC) and the University Laboratory Animal Research at The Ohio State University.

Cell Culture and Therapeutic Agents. Human pancreatic cancer cell lines AsPC-1 (CRL-1682) and MIA PaCa-2 (CRL-1420) were purchased from the American Type Culture Collection (ATCC) and cultured in RPMI1640 and DMEM medium (Sigma) as indicated by the manufacturer, supplemented with 10% fetal bovine serum (FBS, Cat. #A5256701 GIBCO, ThermoFisher), 1% Penicillin/Streptomycin Solution 100X (Euroclone, Cat #ECB3001, Italy). All cell lines were maintained in 37 °C with 5% CO2.For organoid samples, PDAC PDO #23, #6, #2, and #9 were established and cultured as previously described (36).

KRAS^{G12D} inhibitor MRTX-1133 (Cat. # HY-134813), AP-1 inhibitor T-5224 (Cat. # HY-12270), and Gemcitabine (dFdC- Cat # HY-17026) were obtained from MedChemExpress. Cisplatin (CDDP) was purchased from Selleckchem (Cat. # S1166), while U0126 from Sigma-Aldrich (Cat. # 662005). For in vitro studies, all drugs were dissolved in DMSO as indicated by the manufacturer's instruction.

Generation of Stable FRA2^{KO} Clones. To generate FRA2^{KO} clones, CRISPR/Cas-9 technology was used. Stable AsPC-1 FRA2^{KO} pool was obtained by transduction with lentiviral particles (LV01 U6- gRNA:ef1a-puro-2A-Cas9-2A-tGFP, by Sigma-Aldrich). Experimental details are reported elsewhere (18).

Generation of KRASi-res AsPC-1 Cells. KRASi-res AsPC-1 cells were established by continuous exposure of parental AsPC-1 cells to escalating concentrations of the KRAS^{G12D} inhibitor MRTX-1133. Cells were initially treated with 1 nM of MRTX-1133, and the concentration was progressively increased to 50 nM over a 30-d period. Cells were cultured under drug pressure with medium renewed every 72 h and viability monitored by phase-contrast microscopy. Resistant populations were maintained in 50 nM MRTX-1133.

MTS Cell Proliferation and Dose–Response Curves. KRASi-res, FRA2^{KO}, and FRA2^{WT} AsPC-1 cells were seeded into a 96-well culture plate (2,500 cells/well) and treated with increasing doses of MRTX-1133 or U0126. Cell viability was determined at the end of treatment (48 or 72 h, as indicated) using CellTiter 96® AQueous One Solution Cell Proliferation Assay kit (Cat # G3580, Promega).

Western Blot Analysis. Pancreatic cancer cell lines were lysed in Pierce IP lysis buffer (Cat # 8788, ThermoFisher Scientific) supplemented with Halt Protease and Phosphatase Inhibitor Cocktail (Cat # 1861284, ThermoFisher Scientific). PDAC primary tumor samples were homogenized with grinders, on ice. Protein concentration was determined by Protein Assay Dye Reagent Concentrate (Cat. # 5000006, Bio-Rad), following the manufacturer's instructions. Protein lysates were separated in 4 to 20% Criterion™ TGX Stain-Free™ Precast Gel (Cat. # 5678094, Bio-Rad) or 4 to 20% Mini-PROTEAN® TGX Stain-Free™ Precast Gel (Cat. # 4568093) and transferred onto a nitrocellulose membrane (Protran, Cat# 10600001, Amersham, UK). Membranes were incubated at 4 °C overnight with the indicated primary antibodies: anti-Vinculin (sc-25336, Santa Cruz Biotechnology), anti-Fra-2 (Cat. # 19967, Cell Signaling TechnologySA), anti- É£HA2.X phosphoS139 (EP854) (Abcam 81299), anti-pERK1/2$^{T202/Y204}$ (Cat. # 9101 Cell Signaling Technology), anti-p27 (Cat. # 554069, BD Biosciences). After incubation with appropriate horseradish peroxidase-conjugated secondary antibodies (Cat. # 170-6516 and #170-6515, Biorad), signal was detected using Clarity or Clarity Max Western ECL Substrate (Cat. # 1705061 and #1705062, Biorad).

Chromatin Immunoprecipitation Assay. Parental, U0126-treated, and KRASi-resistant AsPC-1 cells were crosslinked with 1% formaldehyde (Cat. # F79-500, Fisher Chemicals) and chromatin was prepared using MNase enzymatic digestion according to the protocol. Chromatin immunoprecipitation (ChIP) was performed using SimpleChIP Enzymatic Chromatin ImmunoPrecipitation Kit (Magnetic Beads, Cat. # 9005S, Cell Signaling Technology). The chromatin samples obtained were incubated at 4 °C overnight with the following antibodies: normal rabbit IgG

(Cat. # 2729, Cell Signaling technology), anti-Fra-2 (Cat. # 19967, Cell Signaling Technology) and anti-H3 (Cat. # 4620, Cell Signaling Technology) as positive control. Immunoprecipitated chromatin was purified and analyzed by the real-time quantitative PCR using SimpleChIP Universal qPCR Master Mix (Cat. # 88989, Cell Signaling Technology). Data were analyzed with the fold enrichment method compared to an unrelated antibody (normal rabbit IgG).

For ChIP analysis, the following primers were used: MTOR sequence1 (Fw: CTGAGGCGGAAGAATCAC'; Rev: AGATAGGATCTCACTCTATTACCC-3'); MTOR sequence2 (Fw: CTTCACCACTCAACACAGAG; Rev: TTGGGACATGGAATTGGTAAG); IGF1R (Fw: CATCCTACCCGATTGTTTGAG; Rev: CCTTAATGTGGTCCGGTTTC). IGF1R primers were previously validated and used in our earlier study (18).

RNA Isolation and Quantitative Real-Time PCR. RNA isolation and quantitative Real-time PCR were performed as already described (18). Briefly, total RNA was isolated from cell lines and primary tumor samples using TRIzol™ Reagent (Cat. # 15596026, Invitrogen), following the instructions provided by the manufacturer. Primary tumor tissues from mice were fragmented with grinders on ice. RNA was extracted from 42 paraffin-embedded PDAC samples using RecoverAll™ Total Nucleic Acid Isolation (Cat. # AM1975, Invitrogen by ThermoFisher Scientific), according to the manufacturer's instructions. For organoid samples, PDO #23, #6, #2, and #9 were dissociated into single cells as previously described (36); then, total RNA was isolated using TRIzol™ Reagent and by the column-based miRNeasy kit (cat # 217084, Qiagen), following the manufacturer's protocol. RNA was retrotranscribed using the High-Capacity cDNA Reverse Transcription Kit (Cat. # 4368813, Applied Biosystems, ThermoFisher Scientific). For RT-qPCR, TaqMan Fast Advanced Master mix (Cat. # 4444556, ThermoFisher Scientific) was used to detect mRNA expression using the following TaqMan® gene expression assays (ThermoFisher Scientific) of human FOSL2/FRA2 (Assay ID Hs01050117_m1), human mTOR (Assay ID Hs00234508_m1); human ACTB (Assay ID Hs03023943_g1) and human GAPDH (Assay ID Hs02786624_g1) were used as normalizers.

In Vivo Experiments (Xenograft Mice). To evaluate the tumor growth and onset of PDAC cells, primary tumors were established by subcutaneous injection of 1.5×10^6 FRA2^{WT} (16 mice) and Fra-2^{KO} (16 mice) AsPC-1 cells into the flanks of female athymic xenograft mice (The Jackson Laboratory). At the tumor onset (Day 0), mice were randomly distributed in four different cohorts: untreated, KRAS inhibitor, AP-1 inhibitor, and combinatorial treatment (Combo). KRAS inhibitor group of mice (n = 4) was treated intraperitoneally (IP) and twice a day with 10 mg/kg of MRTX-1133 resuspended in a solution with the following composition: 10% DMSO, 40% PEG300, 5% Tween-80 and 45% saline; the AP-1 inhibitor group of mice (n = 4) was treated orally and daily with 30 mg/kg of T-5224 resuspended in 10% PVP (polyvinylpyrrolidone) solution; the combo group (n = 4) was treated intraperitoneally (IP), orally or both with MRTX-1133 and T-5224, twice a day and daily respectively; the untreated group (n = 4) was treated with vehicle alone. Growth of primary tumors was monitored by measuring tumor width (W) and length (L) with a caliper as indicated in Fig. 2*A* and calculating tumor volume based on the formula: Tumor volume (mm3) = $(W^2 \times L)/2$.

Histological Analysis and Immunohistochemistry. At the endpoint, histological analyses were performed as previously described (18). Briefly, PDAC tumors from flanks of female athymic xenograft mice were fixed in neutral-buffered formalin 10% for 72 h and processed for standard paraffin embedding. Histological sections (5 μm thick) were made from the paraffin blocks. Routine deparaffinization of murine samples mounted on positive charge slides was carried out according to standard procedures, followed by rehydration through serial ethanol treatments. Slides were immersed in citrate buffer [0.01 M sodium citrate (pH 6.0)] and heated in a microwave oven at 600 W (three times for 5 min each) to enhance antigen retrieval. Endogenous peroxidase was blocked with 0.3% hydrogen peroxide in methanol for 30 min. Sections were immunostained with Ki-67 (Cat. # NBP2- 54791, Novus Bio) antibodies according to the manufacturer's protocol and standardized procedures. Images were collected with Nikon eclipse 600. The histological evaluation of Ki-67 expression was assessed as the percentage of moderately/highly positive neoplastic cells counted in 4 random fields.

Bioinformatics Analysis. From KRASi-res, parental and FRA2^{KO} AsPC-1 cells, treated or not with MRTX-1133, RNA was collected and isolated with TRIzol, RNA clean-up, and concentration kit (Cat. # 23600, Norgen Biotek Corp, Canada). Total RNA was treated with RNase-free DNase I Kit (Cat. # 25710, Norgen Biotek Corp, Canada), to avoid DNA contamination. Transcriptome analysis was conducted on two different samples per condition and was performed with Clariom™ S Assay, Human (ThermoFisher Scientific). The analysis for Clariom™ S Human Affymetrix panel of >21 K genes was carried out by Transcriptome Analysis Console software (TAC v4 - Thermo Fisher Scientific) and it consists of three main steps: 1) data quality control; 2) normalization (signal space transformation robust multiple-array average); 3) differentially expression analysis employing the eBayes method from limma R package included in TAC software. Volcano plot (Fig. 4*A*) was generated by using *EnhancedVolcano* R package (v1.20.0). Functional enrichment analyses were performed by using Ingenuity® Pathway Analysis (IPA®) software (v90348151). Data of FRA2 and MTOR expression were downloaded from cBioPortal resource (37, 38) (TCGA, GDC) (https://www.cbioportal.org) (Fig. 4*B*) and filtered to retain only pancreatic ductal adenocarcinoma samples. To identify highly- and low expressed genes in the dataset, mean expression levels were calculated for each gene across all samples. Data manipulation and preprocessing were performed using dplyr (v 1.1.4) and tidyverse (v 2.0.0) in R. Spearman correlation coefficients between FOSL2 (FRA2) expression and all detected genes across the cohort was computed and the ranked correlation list was used as input for Gene Set Enrichment Analysis (GSEA) (*SI Appendix*, Fig. S1). Hallmark gene sets were retrieved using the msigdbr package (v 25.1.1) and enrichment analysis was performed using clusterProfiler package (v 4.10.1).

For RNA sequencing of PDAC PDOs, RNA was isolated as previously indicated in the "RNA isolation" section. The libraries were obtained using poly(A) enrichment with TrueSeq Stranded mRNA Library Prep kit (Illumina) and sequenced to a depth of 30 M fragments and 150 base paired end reads on an Illumina NextSeq 500 sequencer. Analyses were performed following the procedure described (36): Reads were aligned to the GRCh38 genome using STAR (v2.7), and the transcripts were quantified with RSEM (v1.3.3). For downstream analyses, the raw counts were normalized using the "vst" function of the DESeq2 R package. Genes that have at least 5 counts in at least 3 samples across all PDOs were removed before normalization. Gene set variation analysis (GSVA) was performed on vst-normalized data with the gsva R package, using as input HALLMARK gene sets collection retrieved from msigdb R package. PDOs were annotated as classical and quasi-mesenchymal subtypes according to Moffitt classification (39).

Statistical Analysis. Graphs and statistical analyses were performed using PRISM (version 9, GraphPad, Inc.). In all experiments, differences were considered significant when P-value was < 0.05. Statistical analyses including unpaired t test, two-way ANOVA, and Spearman correlation test were used as appropriate and as specified in the legend of each figure.

Data, Materials, and Software Availability. All raw data that support the findings of this study have been submitted to the NCBI Gene Expression Omnibus (GEO; https://www.ncbi.nlm.nih.gov/geo/) under accession number GSE318496 (22). All data reported in this manuscript are available upon reasonable request.

ACKNOWLEDGMENTS. We are grateful to the patients who participated in this study. We thank the Genomic Shared Resource at The Ohio State University Comprehensive Cancer Center (OSU CCC), supported by the Cancer Center Support Grant P30CA016058, for conducting the Affymetrix microarray assays, in particular Dr. Paolo Fadda. Figs. 1*H* and 2*A* of this manuscript were realized by using the software BioRender.com. This work was supported by AIRC Start-Up Grant #30656 to G.L.R.V.; V.C. is supported by AIRC Investigator Grant #28801.

Author affiliations: [a]Department of Clinical and Molecular Medicine, Faculty of Medicine and Psychology, Sapienza University of Rome, Rome 00189, Italy; [b]Department of Cancer Biology and Genetics and Comprehensive Cancer Center, The Ohio State University, Columbus, OH 43210; [c]Department of Medical and Surgical Sciences, Fondazione Policlinico Universitario Agostino Gemelli Istituto di Ricovero e Cura a Carattere Scientifico, Rome 00136, Italy; [d]Department of Diagnostic, Clinic and Public Health Medicine, University of Modena and Reggio Emilia, Modena 41100, Italy; [e]Surgical, Medical and Dental Department of Morphological Sciences related to Transplant, Oncology and Regenerative Medicine, Hepato-Pancreato-Biliary Surgery and Liver Transplantation Unit, University of Modena and Reggio Emilia, Modena 41100, Italy; [f]Department of Engineering for Innovation Medicine, University of Verona, Verona 37134, Italy; and [g]Division of Molecular Oncology, Centro di Riferimento Oncologico di Aviano, Istituto di Ricovero e Cura a Carattere Scientifico, National Cancer Institute, Aviano 33081, Italy

Author contributions: C.M.C. and G.L.R.V. designed research; E.T., C.D., F.L., G.P., M.C., E.D.R., A.S., R.C., and G.L.R.V. performed research; G.P., C.C., G.N., E.P., L.R.B., and D.P. contributed new reagents/analytic tools; E.T., C.D., F.L., G.P., M.C., G.N., E.P., E.D.R., A.S., P.M., V.C., B.B., G.B., A.V., C.M.C., and G.L.R.V. analyzed data; and E.T., C.D., C.M.C., and G.L.R.V. wrote the paper.

1. W. Park, A. Chawla, E. M. O'Reilly, Pancreatic cancer: A review. *JAMA* **326**, 851–862 (2021).
2. C. Norton *et al.*, *KRAS* mutation status and treatment outcomes in patients with metastatic pancreatic adenocarcinoma. *JAMA Netw. Open.* **8**, e2453588 (2025).
3. O. Strobel, J. Neoptolemos, D. Jäger, M. W. Büchler, Optimizing the outcomes of pancreatic cancer surgery. *Nat. Rev. Clin. Oncol.* **16**, 11–26 (2019).
4. T. Conroy *et al.*, Pancreatic cancer: ESMO clinical practice guideline for diagnosis, treatment and follow-up★. *Ann. Oncol.* **34**, 987–1002 (2023).
5. T. Golan *et al.*, Maintenance olaparib for germline BRCA-mutated metastatic pancreatic cancer. *N. Engl. J. Med.* **381**, 317–327 (2019).
6. Y. Jiang, D. P. S. Sohal, Pancreatic adenocarcinoma management. *JCO Oncol. Pract.* **19**, 19–32 (2023).
7. L. Huang, Z. Guo, F. Wang, L. Fu, *KRAS* mutation: From undruggable to druggable in cancer. *Sig. Transduct. Target. Ther.* **6**, 386 (2021).
8. J. Canon *et al.*, The clinical *KRAS*(G12C) inhibitor AMG 510 drives anti-tumour immunity. *Nature* **575**, 217–223 (2019).
9. F. Skoulidis *et al.*, Sotorasib for lung cancers with *KRAS* p. G12C mutation. *N. Engl. J. Med.* **384**, 2371–2381 (2021).
10. M. Drosten, M. Barbacid, Targeting *KRAS* mutant lung cancer: Light at the end of the tunnel. *Mol. Oncol.* **16**, 1057–1071 (2022).
11. X. Wang *et al.*, Identification of MRTX1133, a noncovalent, potent, and selective KRASG12D inhibitor. *J. Med. Chem.* **65**, 3123–3133 (2022).
12. J. Hallin *et al.*, Anti-tumor efficacy of a potent and selective non-covalent KRASG12D inhibitor. *Nat. Med.* **28**, 2171–2182 (2022).
13. J. Dilly *et al.*, Mechanisms of resistance to oncogenic *KRAS* inhibition in pancreatic cancer. *Cancer Discov.* **14**, 2135–2161 (2024).
14. R. Eferl, E. F. Wagner, AP-1: A double-edged sword in tumorigenesis. *Nat. Rev. Cancer* **3**, 859–868 (2003).
15. G. L. Rampioni Vinciguerra *et al.*, Role of Fra-2 in cancer. *Cell Death Differ.* **31**, 149 (2023), 10.1038/s41418-023-01248-4.
16. L. Bakiri *et al.*, Liver cancer development driven by the AP-1/c-Jun~Fra-2 dimer through c-Myc. *Proc. Natl. Acad. Sci.* **121**, e2404188121 (2024).
17. N. Gupta *et al.*, ERO1α promotes hypoxic tumor progression and is associated with poor prognosis in pancreatic cancer. *Oncotarget* **10**, 5970–5982 (2019).
18. G. L. Rampioni Vinciguerra *et al.*, Nutrient restriction-activated Fra-2 promotes tumor progression via IGF1R in miR-15a downmodulated pancreatic ductal adenocarcinoma. *Signal Transduct. Target. Ther.* **9**, 31 (2024).
19. Z. Li *et al.*, LncRNA UCA1 mediates resistance to cisplatin by regulating the miR-143/FOSL2-signaling pathway in ovarian cancer. *Mol. Ther. Nucleic Acids* **17**, 92–101 (2019).
20. G. L. Rampioni Vinciguerra *et al.*, Role of the miR-301a/Fra-2/GLIPR1 axis in lung cancer cisplatin resistance. *Sig. Transduct. Target Ther.* **8**, 1–4. (2023)
21. W. H. Chen *et al.*, Human pancreatic adenocarcinoma: In vitro and in vivo morphology of a new tumor line established from ascites. *In Vitro* **18**, 24–34 (1982).
22. G. L. Rampioni Vinciguerra, G. Nigita, Data From "Fra2 role in PDAC response under MRTX-1133 treatment". GEO. https://www.ncbi.nlm.nih.gov/geo/query/acc.cgi?acc=GSE318496. Deposited 13 April 2026.
23. A. D. Rouillard *et al.*, The harmonizome: a collection of processed datasets gathered to serve and mine knowledge about genes and proteins. *Database (Oxford)* **2016**, baw100 (2016).
24. H. Gazon, B. Barbeau, J.-M. Mesnard, J.-M. Peloponese, Hijacking of the AP-1 signaling pathway during development of ATL. *Front. Microbiol.* **8**, 2686 (2018).
25. A. Subramanian *et al.*, Gene set enrichment analysis: A knowledge-based approach for interpreting genome-wide expression profiles. *Proc. Natl. Acad. Sci.* **102**, 15545–15550 (2005).
26. E. Gurreri *et al.*, *KRAS*-dependency in pancreatic ductal adenocarcinoma: Mechanisms of escaping in resistance to *KRAS* inhibitors and perspectives of therapy. *Int. J. Mol. Sci.* **24**, 9313 (2023).
27. S. Zhang *et al.*, Chromatin accessibility uncovers KRAS-driven FOSL2 promoting pancreatic ductal adenocarcinoma progression through up-regulation of CCL28. *Br. J. Cancer* **129**, 426–443 (2023), 10.1038/s41416-023-02313-y.
28. H. Hua, Q. Kong, J. Yin, J. Zhang, Y. Jiang, Insulin-like growth factor receptor signaling in tumorigenesis and drug resistance: A challenge for cancer therapy. *J. Hematol. Oncol.* **13**, 64 (2020).
29. T. Isermann, C. Sers, C. J. Der, B. Papke, KRAS inhibitors: Resistance drivers and combinatorial strategies. *Trends Cancer* **11**, 91–116 (2025).
30. C. Fedele *et al.*, SHP2 inhibition diminishes KRASG12C cycling and promotes tumor microenvironment remodeling. *J. Exp. Med.* **218**, e20201414 (2020).
31. H. Kitai *et al.*, Combined inhibition of KRASG12C and mTORC1 kinase is synergistic in non-small cell lung cancer. *Nat. Commun.* **15**, 6076 (2024).
32. K. K. Mahadevan *et al.*, *KRASG12D* inhibition reprograms the microenvironment of early and advanced pancreatic cancer to promote *FAS*-mediated killing by *CD8*+ T cells. *Cancer Cell* **41**, 1606–1620.e8 (2023).
33. S. B. Kemp *et al.*, Efficacy of a small-molecule inhibitor of KrasG12D in immunocompetent models of pancreatic cancer. *Cancer Discov.* **13**, 298–311 (2023).
34. C. D. Yao *et al.*, AP-1 and TGFß cooperativity drives non-canonical hedgehog signaling in resistant basal cell carcinoma. *Nat. Commun.* **11**, 5079 (2020).
35. H. Makino *et al.*, A selective inhibition of c-Fos/activator protein-1 as a potential therapeutic target for intervertebral disc degeneration and associated pain. *Sci. Rep.* **7**, 16983 (2017).
36. E. Fiorini *et al.*, MYC ecDNA promotes intratumour heterogeneity and plasticity in PDAC. *Nature* **640**, 811–820 (2025).
37. E. Cerami *et al.*, The cBio cancer genomics portal: An open platform for exploring multidimensional cancer genomics data. *Cancer Discov.* **2**, 401–404 (2012).
38. J. Gao *et al.*, Integrative analysis of complex cancer genomics and clinical profiles using the cBioPortal. *Sci. Signal.* **6**, pl1 (2013).
39. R. A. Moffitt *et al.*, Virtual microdissection identifies distinct tumor- and stroma-specific subtypes of pancreatic ductal adenocarcinoma. *Nat. Genet.* **47**, 1168–1178 (2015).